ELSEVIER

Biophysical Chemistry 64 (1997) 111–119

Biophysical Chemistry

Thermal unfolding of the N-terminal RNA binding domain of the human U1A protein studied by differential scanning calorimetry

Jirong Lu, Kathleen B. Hall *

Department of Biochemistry and Molecular Biophysics, Washington University School of Medicine, St. Louis, MO 63110, USA

Received 28 June 1996; revised 7 August 1996; accepted 7 August 1996

Abstract

Thermal unfolding of the N-terminal RNA binding domain of human U1A protein (RBD1) and several variants has been observed by differential scanning calorimetry. Unfolding of the 95 amino acid domain is reversible and cooperative between pH 2.0 and 2.8 in 40 mM glycine, with a heat capacity for the transition of 1.2 kcal $mol^{-1} K^{-1}$, and an unfolding free energy of 4.0 kcal mol^{-1} at pH 2.3 and 25°C. At higher pH, thermal unfolding is irreversible. In contrast, unfolding of the protein by guanidine hydrochloride denaturation at pH 2.3 and pH 7.0 is reversible, with unfolding free energies of 6.6 and 9.0 kcal mol^{-1}, respectively. DSC experiments show that RBD variants in which the N-terminal tail is truncated, or in which a functional loop is substituted, have altered unfolding free energies but little variation in their heat capacities of transition.

Keywords: Protein unfolding; RNA binding domain; Human U1A; Differential scanning calorimetry

1. Introduction

The RNA binding domain (RBD), also known as RNA recognition motif (RRM) or ribonucleoprotein motif (RNP), is a small 90 amino acid domain with an α/β sandwich topology. It is possibly the most common RNA binding motif, with over 70 examples identified by the sequence and position of two consensus regions, the RNP-1 octamer and the RNP-2 hexamer [1]. These two conserved sequences comprise two of the four β-strands of the four-stranded anti-parallel β-sheet characteristic of these proteins, which all seem to share a $\beta\alpha\beta$-$\beta\alpha\beta$ secondary structure. The two α-helices are packed against the β-sheet, with the interface forming the hydrophobic core of the protein. There are a number of conserved hydrophobic residues interspersed throughout the sequence [1,2], many of which are involved in the formation of the hydrophobic core.

The tertiary structure of several of these proteins has been solved, including the human U1A N-terminal RBD1 by X-ray crystallography and NMR [3,4], the C-terminal RBD2 by NMR (Lu & Hall, in preparation), the hnRNP C domain by NMR [5], and the second RBD of *Drosophila* sxl [6]. In addition, the structure of the U1A RBD1:RNA cocrystal has been described [7], showing the contacts between the RNA hairpin and the protein. The surface of the β-sheet is the primary RNA binding surface in these proteins [7–9].

* Corresponding author.

PII S0301-4622(96)02212-0

The ribbon diagram of the human U1A RBD1 is shown in Fig. 1, together with its amino acid sequence. Many mutations have been made in this protein, with the goal of identifying the residues important for RNA binding [10–16]. However, given that there are so many apparently similar RBDs that recognize such a variety of RNA sequences and structures, it is also important to understand how these proteins differ with respect to their structure, energetics, and folding. The contribution of conserved and variable amino acids to protein stability is also related to RBD function, through specific interactions with RNA as well as through protein dynamics and conformational flexibility. Therefore, we have used differential scanning calorimetry (DSC) to investigate the thermal unfolding of the human U1A RBD1 and several variants, in order to identify those amino acids that contribute to protein stability and structural integrity. Because unfolding of this RBD by guanidine hydrochloride is fully reversible and proceeds without any detectable population of intermediates [15], and because it is also one of the few RBD domains that is soluble, it is especially valuable as a model system for these proteins.

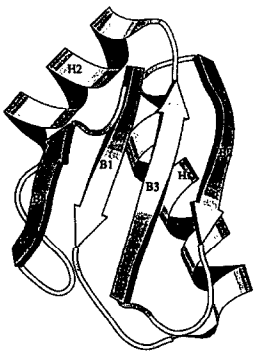

RBD1 (1-51) MAVPETRPNHTIYINNLNEKIKKDELKKSLYAIFSQFGQILDILVSRSLKM

RBD1 (52-102) RGQAFVIFKEVSSATNALRSMQGFPFYDKPMRIQYAKTDSDIIAKMKGTFV

Fig. 1. Tertiary structure and amino acid sequence of the N-terminal RNA binding domain of human U1A protein with secondary structure indicated. The three-dimensional structure of RBD1(95A) (from reconstruction of van Gelder et al. [30], using the structure of Nagai et al. [3]) is shown as a ribbon diagram.

2. Materials and methods

2.1. Sample preparation

All proteins were overproduced and purified following a standard procedure [17]. The construct containing 1–102 amino acids of the human U1A protein is referred to as wildtype RBD1(102A). RBD1(95A) is the construct containing amino acids 1–95. RBD1(8–99) contains amino acids 8–99 with Arg7 and Asn8 replaced by Met and Ala, respectively. RBD1(Δloop3) is 102A with the six amino acids of loop3 (Ser46-Arg47-Ser48-Leu49-Lys50-Met51) replaced with four residues (Val-Pro-Gly-Arg), corresponding to loop3 of the U1A C-terminal RBD2.

Buffers used for DSC were 40 mM glycine–HCl between pH 2.0 and 3.4. About 1.5–2.5 mg of the proteins were dialyzed extensively against buffers using Spectrapor 2 dialysis membrane with MWCO 6000–8000 Da. For comparison of the stability of mutant RBDs, samples were dialyzed in the same container to ensure identical buffer conditions, and this final dialysate was used as a reference solution. The concentration of protein was determined by UV absorption at 280 nm, using $\epsilon = 5120\ \mathrm{cm}^{-1}\ \mathrm{M}^{-1}$, based on four tyrosine residues in the protein [17].

2.2. Circular dichroism spectroscopy

Circular dichroism spectra were measured using a Jasco-J600 spectropolarimeter. Spectra were measured from 250 to 200 nm with a 0.1-cm pathlength cell using 30 μM protein samples. Guanidine hydrochloride unfolding of RBD1(102A) was carried out in 40 mM glycine buffer at pH 2.3. The ellipticity of individual samples at 220 nm was time-averaged for 200 time points, then duplicate experiments were averaged together. These averaged values of ellipticity were fit with a linear extrapolation model, $\Delta G_d = \Delta G_d^\circ - mC$ [18,19], where C is the concentration of GdnHCl and m is the slope at the transition, using Kaleidegraph software as described previously [15]. The concentration of GdnHCl in the stock solution was determined by refractive index [19].

2.3. Differential scanning calorimetry and data analysis

Calorimetric measurements were carried out on a MicroCal MC-2 scanning calorimeter. In all measurements, the heating rate was 1°C min^{-1}. DSC data were normalized for concentration after subtraction of the instrument baseline. The data were then fit with a two-state model to obtain T_m, $\Delta H_d(T_m)$, and a temperature-dependent ΔC_p, using non-linear least squares analysis with Mathcad (MathSoft Inc) software, allowing both the upper and lower baselines to float independently. The linear portion of the pre- and post-transition baselines are expressed in cal $mol^{-1}K^{-1}$, as $C_p(N) = b_0 + b_1(T - T_m)$ and $C_p(D) = b_2 + b_3(T - T_m)$. Temperature dependence of the heat capacity for the (N) native (b_1) and (D) denatured state (b_3) was determined from the linear fit of the baselines for the native and denatured state using the DSC scans at different pH values of RBD1(95A). Errors in the enthalpy and T_m, based on two or three separate experiments with a single protein, are no more than 5%. Errors in the heat capacity are considerably greater, primarily ascribed to variations in the buffer baseline. Errors in these values are estimated to be between 15 and 20%.

3. Results

3.1. RBD1(102A) unfolding at pH 2.3: DSC and GdnHCl

About 1.5 to 2 mg ml^{-1} protein (about 0.2 mM) in 40 mM glycine from pH 2.0 to pH 3.4 was used for DSC. Under these conditions, the protein is monomeric in solution based on NMR analysis and elastic light scattering (data not shown). DSC scans of the thermal denaturation of RBD1(102A) at pH 2.3 are shown in Fig. 2a. As indicated, the denaturation is reversible at this pH; after two consecutive experiments, the protein was estimated to be at least 90% reversible.

As anticipated, the heat capacity of the native protein increases linearly until nearly 40°C, with a slope $\Delta C_p^N(T)/\Delta T = 13$ cal $mol^{-1}K^{-2}$ (1.2×10^{-3} cal $g^{-1}K^{-2}$). Denaturation is accompanied by a large heat capacity change, while in the denatured state

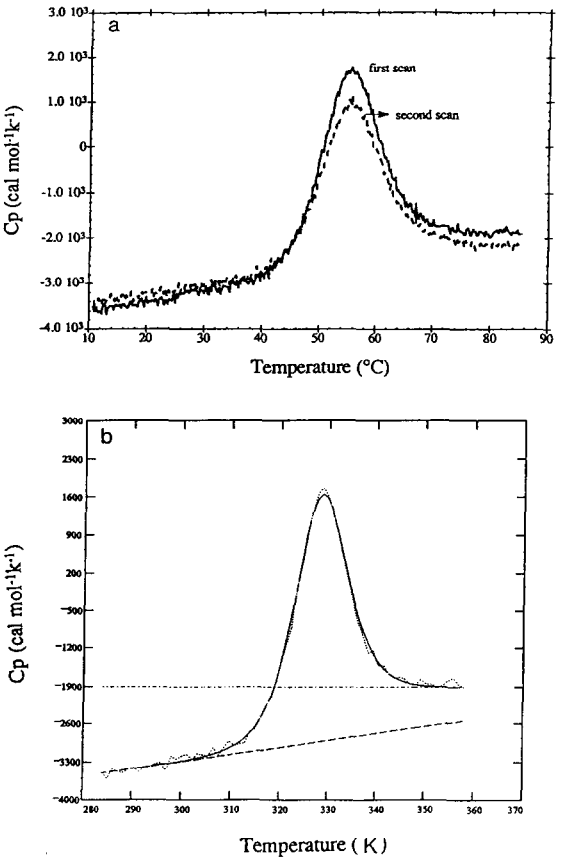

Fig. 2. DSC scans of 2 mg ml^{-1} RBD1(102A) in 40 mM glycine HCl buffer at pH 2.3. The data are normalized for concentration after subtraction of the instrument base line. a. Two successive scans of RBD1(102A). The reversibility of the second scan was estimated to be more than 90% by comparison of the areas under the curve. b. DSC curve for the first scan of RBD1(102A) at pH 2.3. The data are shown as the dotted line. The solid curve is the fit of the data using a two-state model. The dashed lines are the fit of baselines for native and denatured proteins.

there is no apparent temperature dependence of the heat capacity. NMR spectra taken at different temperatures between 25 and 80°C showed that the protein becomes fully unfolded at 65°C; there is no further change in the NMR spectrum from 65 to 80°C at pH 2.3 (data not shown), indicating that the denatured state observed in the DSC represents the fully unfolded state of the protein. The heat capacity for unfolding can be determined by a fit of the data, as shown in Fig. 2b, using a two-state model. As given in Table 2, at pH 2.3, at the midpoint of the

unfolding transition ($T_m = 56.6°C$), $\Delta H_d(T_m) = 58.1$ kcal mol^{-1}, $\Delta S_d(T_m) = 176$ cal mol^{-1}K^{-1}, and $\Delta C_p(T_m) = 982$ cal mol^{-1}K^{-1}. In order to compare to the unfolding free energy determined by guanidine denaturation, the free energy of unfolding at 25°C was calculated to be 4 kcal mol^{-1}, using the following relations and the temperature-dependent ΔC_p

$$\Delta H_d(T) = \Delta H_d(T_m) + \int_{T_m}^{T} \Delta C_p(T)dT \quad (1)$$

$$\Delta S_d(T) = \Delta S_d(T_m) + \int_{T_m}^{T} \Delta C_p(T)d\ln T \quad (2)$$

$$\Delta G_d(T) = \Delta H_d(T) - T\Delta S_d(T) \quad (3)$$

Previous structural, thermodynamic, and dynamic characterization of the protein was done at higher pH [3,4,15]. To compare the secondary structure of the protein in these different conditions, the CD spectra were acquired at pH 2.3 and pH 7.0. The spectra are nearly identical, as illustrated for one of the variants, RBD1(Δloop3) in Fig. 3, indicating that the secondary structure content of the protein does not change in this pH range.

Thermodynamic characterization of RBD1(102A) determined the unfolding free energy using guanidinium hydrochloride denaturation at pH 7. With this method, $\Delta G_d^\circ = 9.0 \pm 0.6$ kcal mol^{-1}, with a midpoint GdnHCl concentration of 3.75 M (data not shown). These experiments were repeated at pH 2.3 in 40 mM glycine HCl, to facilitate comparison with the DSC data. Those results are shown in Fig. 4,

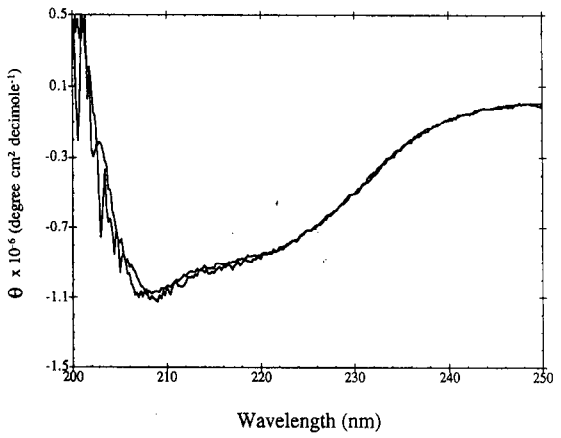

Fig. 3. Circular dichroism spectra of 30 μM RBD1(Δloop3) in 40 mM glycine HCl (pH 2.3), and 50 mM NaCl, 10 mM sodium cacodylate (pH 7.0), 22°C.

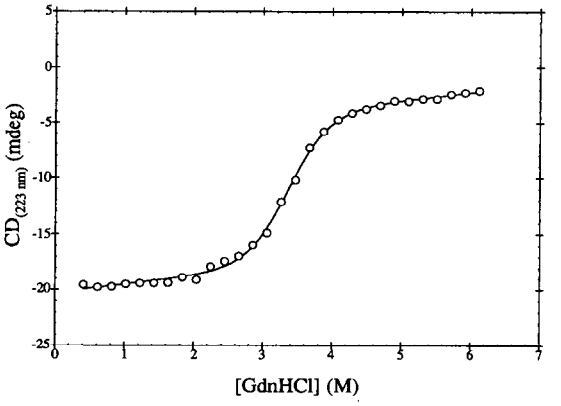

Fig. 4. Ellipticity at 223 nm as a function of GdnHCl concentration for RBD1(102A) in the presence of 40 mM glycine HCl at pH 2.3, 22°C. The solid line is the nonlinear least-square best fit to the data using the linear extrapolation model. Data sets used for calculation of ΔG° are the averages of duplicate experiments with 30 separate denaturant concentrations.

with the fit to the data based on the linear extrapolation model to give $\Delta G_d^\circ = 6.6 \pm 0.4$ kcal mol^{-1} with a midpoint GdnHCl concentration of 3.38 M. The difference in unfolding free energy as measured by guanidine hydrochloride denaturation, from 9.0 kcal mol^{-1} at pH 7.0 to 6.6 kcal mol^{-1} at pH 2.3, indicates that electrostatic effects contribute a substantial fraction of the overall stability of the protein over this pH range. The differences between the values of ΔG_d° obtained from guanidine denaturation at pH 2.3 (6.6 kcal mol^{-1}) and from DSC (4.0 kcal mol^{-1}) reflect interaction of the denaturant with the protein as well as errors from extrapolation.

3.2. Unfolding of RBD1(95A) vs. pH

Thermal unfolding of RBD1(95A) was measured as a function of pH to determine the range of reversible denaturation and to obtain the average heat capacity of denaturation. DSC scans at pH 2.0, 2.7, 3.0, and 3.2 are shown in Fig. 5. The denaturation temperature increases with increasing pH, while the temperature-dependent heat capacity of the native form is independent of pH; the heat capacity of the unfolded form has no temperature dependence at any pH shown. However, at higher pH, the heat capacity of the unfolded protein appears to decrease precipitously, probably due to aggregation. In 25 mM KCl,

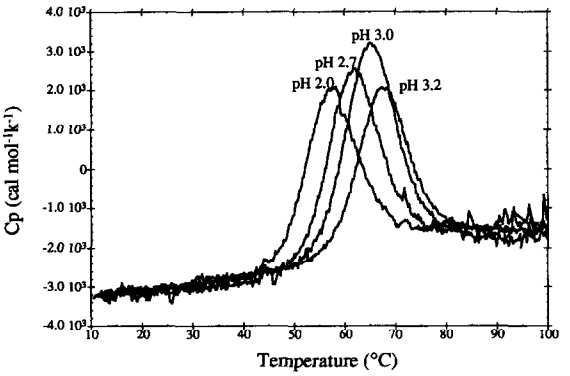

Fig. 5. DSC scans for 2 mg ml^{-1} RBD1(95A) in 40 mM glycine HCl at different pH values.

20 mM potassium phosphate at pH 5.5, thermal unfolding is irreversible, and the protein precipitates upon denaturation (data not shown).

The T_m, $\Delta H_d(T_m)$, and ΔC_p of unfolding from pH 2.0 to pH 3.4 are given in Table 1, and the plot of the unfolding enthalpy vs. denaturation temperature is shown in Fig. 6a. The slope of this line, determined from a linear least square fit of the data, gives the average heat capacity of unfolding to be 1.2 ± 0.1 kcal $mol^{-1} K^{-1}$. The data from the pH 3.0, 3.2, and 3.4 experiments are not included in this analysis, since their dramatic decrease in heat capacity indicates that the state of the protein has changed, probably signifying a loss of reversibility. This value of $\Delta C_p = 1.2$ kcal $mol^{-1} K^{-1}$ is a property of this

Table 1
The pH dependence of the denaturation of RBD1(95A)

pH	T_m /°C	$\Delta H_d(T_m)$/ kcal mol^{-1}	$\Delta C_p(T_m)$/ cal $mol^{-1} K^{-1}$
2.00	55.3	57.9	1163
2.30	57.2	58.4	1166
2.50	58.9	61.2	1275
2.70	60.9	62.5	1153
2.85	62.8	65.8	850
3.00	64.8	65.9	616
3.20	69.0	69.4	121
3.40	70.5	69.8	258

Protein in 40 mM glycine HCL buffer. $\Delta H_d(T_m)$ and T_m from the fit of the DSC data to a two-state model. Errors in T_m and ΔH_d estimated at 5%, and at 15–20% for ΔC_p, based on multiple experiments.

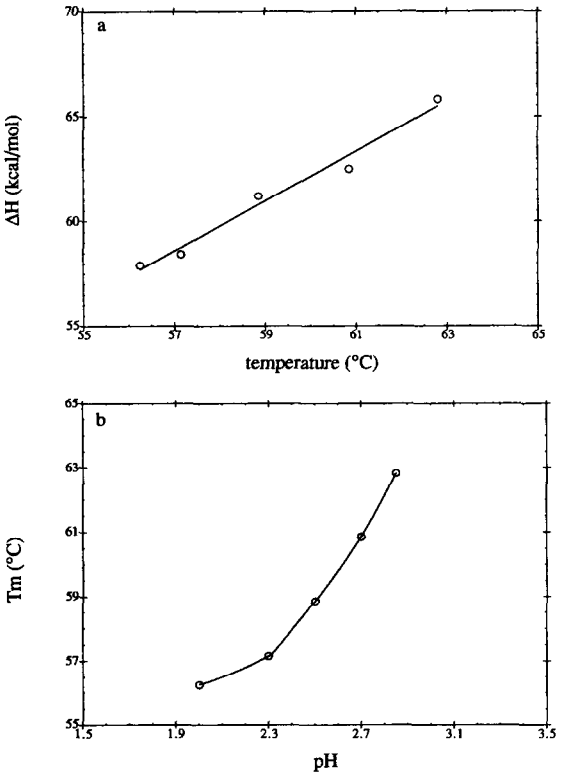

Fig. 6. Variation of T_m, $\Delta H_d(T_m)$ with pH for RBD1(95A). a. $\Delta H_d(T_m)$ as a function of T_m. Linear regression analysis gives $\Delta C_p = 1.2 \pm 0.1$ kcal $mol^{-1} K^{-1}$ ($r = 0.990$). b. Melting temperature as a function of pH. The solid curve is the interpolation of the data points.

RBD, and can be used as a reference value for comparison to other variant RBD proteins.

The T_m as a function of pH is plotted in Fig. 6b. The stability of the protein increases significantly with the increase in pH; the T_m increases about 10°C from pH 2.0 to pH 3.0. From the linear portion of the curve, it is possible to estimate the number of protons taken up ($\Delta \nu$) by the protein during denaturation, using the relation [20]

$$\Delta \nu = \frac{\Delta H_{cal}}{2.303 R T_m^2} \times \frac{dT_m}{dpH} \quad (4)$$

For this protein, $\Delta \nu$ is about 1.2 from pH 2.3 to pH 2.85. This small uptake of protons may be due to the presence in the native protein of carboxyl groups with low pK values.

Table 2
Thermodynamics of variant RBD proteins

Protein	T_m/ °C	ΔH_d/ kcal mol^{-1}	ΔS_d/ cal mol^{-1} K^{-1}	$\Delta C_p/(T_m)$/ cal mol^{-1} K^{-1}	ΔC_p(56°C)/ cal mol^{-1} K^{-1}	$\Delta\Delta G_d^a$/ kcal mol^{-1}	$\Delta\Delta H_d^a$ (kcal mol^{-1})	$\Delta\Delta S_d^a$ (cal mol^{-1} K^{-1})
RBD1(102A)	56.6	58.1	176	982	982			
RBD1(95A)	57.0	58.6	177	1166	1166	0	0	0
RBD1(8–99)	47.0	40.3	127	952	820	−1.4	−9.6	−25
RBD1(Δloop3)	65.4	57.3	169	810	940	1.4	−8.8	−31

ΔH_d, ΔS_d, ΔC_p of unfolding evaluated at the melting temperature of each protein. Error in ΔH_d estimated at 5%; errors in ΔC_p at 15%.[a] $\Delta\Delta G_d$, $\Delta\Delta H_d$, $\Delta\Delta S_d$ = (Mutant) − RBD1(102A), calculated at 56.6°C according to Eqs. (1)–(3), assuming a temperature-dependent ΔC_p(56.6°C).

3.3. Comparison of the thermodynamic parameters of wildtype RBD1 and variants

Several variants of RBD1(102A) were constructed to determine their thermodynamic contribution to protein stability and their influence on RNA binding. Three regions of the domain were investigated: the C-terminal tail, the N-terminal tail, and loop3 between $\beta 2$ and $\beta 3$. To compare their energetics, thermal unfolding was carried out in 40 mM glycine HCl buffer at pH 2.3, which for RBD1(95A) is in the region where the enthalpy varies linearly with transition temperature (Fig. 6); the assumption made is that this will be true for the other proteins as well. In addition to their measured thermodynamic parameters, the difference in the standard free energies of unfolding for the wildtype RBD1(102A) and mutant proteins ($\Delta\Delta G_d^\circ$) (Eq. (5)) was used to compare the apparent stability of the constructs

$$\Delta\Delta G_d^\circ = \Delta G_d^\circ(\text{variant}) - \Delta G_d^\circ(WT) \qquad (5)$$

$\Delta G_d^\circ(WT)$ is zero at its melting temperature, and positive values of $\Delta\Delta G_d^\circ$ indicate apparent stabilization of the native state of a protein. This difference is evaluated at the transition temperature T_m of RBD1(102A) at pH 2.3 using Eqs. (1)–(3), assuming a temperature-dependent ΔC_p.

Thermodynamic data for these proteins are given in Table 2; they can be compared on the basis of their T_m, ΔH_d, ΔS_d, and ΔC_p values. The denaturation temperatures of 102A and 95A, which differ by seven amino acids at the C-terminus, are nearly identical, as are the heat capacities of their native states and their denaturation heat capacities. The entropy and enthalpy of unfolding are also nearly identical; the heat capacity of transition appears greater for the shorter protein by about 20%, but this is within the error of these determinations. RBD1(8–99), with a shorter N-terminal tail, is destabilized compared to the RBD1(102A) parent. Its melting temperature is nearly 10°C lower than that of the RBD1(102A) construct at this pH, corresponding to a loss of about 1.4 kcal mol^{-1} in the folding free energy of the domain. It has a more favorable enthalpy of unfolding ($\Delta\Delta H_d$), but a less favorable entropy ($\Delta\Delta S_d$), extrapolating to the T_m of 102A. Its heat capacity of transition at 56.6°C is within 15% of that of 102A. The RBD1(Δloop3) variant is nearly 9°C more stable than 102A, corresponding to an increase of 1.4 kcal mol^{-1} in folding free energy. At the transition temperature of the 102A construct, the enthalpy of the RBD1(Δloop3) protein is also more favorable and the entropy is less favorable than for the RBD1(102A), although their heat capacities are comparable. These changes in free energy of folding can be due to the effect of mutation on the native or denatured state, or both.

4. Discussion

4.1. Thermodynamic properties of RBDs

The free energy of unfolding of the RBD1(102A) domain has been characterized by guanidine hydrochloride denaturation as well as differential scanning calorimetry. Both methods show that this α/β sandwich protein is extremely stable, with a T_m of 57°C at pH 2.3, and a midpoint of 3.38 M GdnHCl. The precise values of the unfolding free energy measured by these two methods are in modest agreement; the discrepancy may be attributed to the long extrapolation to 0 M GdnHCl, extrapolation to 25°C, and interaction of the denaturant with the protein. Al-

though chemical denaturation has been used as a preferred method for evaluating unfolding free energy changes of proteins, there are indications that the unfolding ΔG_d may not be a linear function of denaturant [21,22], and there are also instances in which different denaturants do not give the same value of ΔG_d from extrapolation [23–26]. DSC thus appears to be the more reliable method for determination of thermodynamic data for this protein. However, it must also be noted that reversible denaturation requires low pH (pH < 3.0), so that these thermodynamic parameters are not available at higher pH (pH 6–7), where protein activity is measured.

The average heat capacity of denaturation can be obtained from the dependence of the enthalpies of denaturation upon the transition temperature, shown in Fig. 6. For the RBD1(95A), this calculated value of $\Delta C_p = 1.2 \pm 0.1$ kcal mol^{-1} K^{-1} is a property of this protein, and reflects its topology and its amino acid composition (41% aliphatic/11% aromatic/48% polar residues). Presumably all RBDs share this tertiary topology; their amino acid compositions are likewise similar [1], and therefore their heat capacity of denaturation might be expected to be comparable. In the one buffer condition (pH 2.3) used here to compare four RBD constructs, there are significant differences in their stabilities, but not in the heat capacities of transition. To be confident that the values of ΔC_p are characteristic of each construct, the pH dependence of denaturation (enthalpy) must still be determined; this method of obtaining the average ΔC_p seems to be the most reliable for this type of comparative study.

4.2. Effect of N-terminal and C-terminal regions of RBD1 on protein stability

The construct of RBD1 from amino acids 1–102 contains both an N-terminal tail, from amino acids 1 to 9, and a C-terminal tail, from amino acids 91–102. Backbone dynamics, observing ^{15}N relaxation, showed that the first seven amino acids were disordered on the ps–ns time-scale, with order parameters typical of small molecules (Lu & Hall, in preparation). Amino acids 92–98 form an additional α-helix centered around A95, which is thought to interact with sidechains on the surface of the β-sheet to bury hydrophobic residues [4]. However, ^{15}N backbone dynamics measurements show that residues 100–102 are largely disordered, and residues 90–99 have progressively smaller order parameters, indicating less restricted motion (Lu and Hall, in preparation). For these DSC experiments, three constructs are studied that differ in the lengths of their N-terminal or C-terminal tails. Their structures are certain to be very similar, since the hydrophobic core of these proteins has not been altered through mutation or substitution.

In the RBD1(8–99), the first seven amino acids were deleted, and N9 replaced by A9; this construct is less stable than the RBD1(102A). The cause of this destabilization is not apparent, although several possible explanations can be found in the structure. Interactions between residues at the N-terminal end of β1 (amino acids 9–12) and residues from α2 contribute to the stability of the protein, as do interactions between α2 and residues at the C-terminal end of β4, as mutations of Y86 have shown [15]. It is possible that truncation of the N-terminal tail to residue 9 has resulted in more flexibility of the β1 strand, which makes its interactions with α2, β4, and β3 more tenuous. If so, then measurement of the backbone dynamics of this construct should show more disorder in this region. Functionally, this tail can be swapped with that of the U1A C-terminal RBD2 without loss of RNA binding [27]; the RBD1(8–99) construct itself binds RNA with wild-type affinity. Thus the loss of protein stability for RBD1(8-99) is not reflected in its function.

The RBD1(95A) domain presumably lacks the α-helix formed by the C-terminal tail. The energetics and stability of RBD1(102A) and RBD1(95A) are virtually identical at pH 2.3; although the heat capacity differs, it is within the errors attributed to these values. If the C-terminal residues of the domain were packed against the body of the protein, the disruption of this structure might be reflected in the entropy and enthalpy of denaturation; no difference is observed, however. Binding of the RBD1(95A) to RNA is weaker by approximately 30-fold than RBD1(102A) binding, and has a reduced salt dependence [28], indicating that these residues have a functional role.

4.3. Loop3 and protein stability

The size and sequence of loops in RBDs are highly variable [1]. Loop3 in RBD1, which contains

seven residues, has been shown to be critical for binding to the U1 snRNA RNA hairpin [7,11]. This loop is relatively undefined in the crystal structure of the protein, and responds to RNA binding by protruding into the RNA loop where it adopts a 3_{10} helix [7]. ^{15}N NMR backbone dynamics studies in solution have shown that the motional properties of this region are complex; it undergoes some conformational exchange in the ms time-scale. In contrast, loop3 in the U1A C-terminal RBD2 has five residues that show no distinctive backbone dynamics (Lu & Hall, in preparation). RBD2 does not bind RNA [27].

Replacement of the RBD1 loop3 with that of RBD2 in the RBD1(Δloop3) construct stabilizes the domain. Residues in this loop are not conserved among RBDs; in particular, no residue involved in the hydrophobic core of the protein is located in loop3. Based on ^{15}N NMR data for RBD1 and RBD2, we predict that the RBD1(Δloop3) domain will show restricted dynamic motion of loop3, reflecting reduced flexibility. It is possible that the residues in this new shorter loop make novel interactions with other amino acid sidechains or backbone groups, accounting for its higher stability. It is also possible that the shorter loop is packed more tightly against the body of the protein. However, the enthalpy and heat capacity of its unfolding transition are very similar to those of RBD1(102A). It should be noted that RBD2, which has an unfolding free energy of $8.3 + 0.8$ kcal mol^{-1} measured by guanidine hydrochloride denaturation at pH 7.0 [27], is not well-behaved in DSC experiments, because its thermal denaturation cannot be described by a two-state transition (data not shown).

RBD1(Δloop3) binds to the wildtype RNA hairpin with an affinity that corresponds to nonspecific association of RNA by RBD1(102A). This loss of affinity is probably a combination of loss of specific amino acids and loss of conformational flexibility; the higher protein stability does not correspond to tighter RNA binding.

5. Conclusions

The N-terminal RBD1 of the human U1A protein is one of a large class of structurally homologous proteins that bind various RNA targets, yet it is one of the few that are well-behaved in physical studies. In these experiments, thermal unfolding of this domain is shown to be a reversible event that can be monitored by differential scanning calorimetry. Preliminary experiments with three variants of RBD1 show that their enthalpy and T_m can vary significantly, although their heat capacities appear similar; however, there is no correlation between the protein stability and its affinity for the target RNA hairpin. Because the structure of the RBD is known, it may be possible to analyze the effect of mutations in terms of changes in hydrogen bonds and surface area, similar to analysis of larger, more complex proteins such as lysozyme, ribonuclease, or interleukin-1β [29].

Acknowledgements

We thank Tony Pryse for help in use of the DSC instrument and data analysis. This research is supported by the Council for Tobacco Research and the NIH (GM46318 to K.B.H and postdoctoral fellowship GM16739 to J.L).

References

[1] E. Birney, S. Kumar and A.R. Krainer, Nucl. Acids Res., 21 (1993) 5803.
[2] C.G. Burd and G. Dreyfuss, Science, 265 (1994) 615.
[3] K.Nagai, C. Oubridge, T.H. Jessen, J. Li and P.R. Evans, Nature, 348 (1990) 515.
[4] J.M. Avis, F.H.-T. Allain, P.W.A. Howe, G. Varani, K. Nagai and D. Neuhaus, J. Mol. Biol., 257 (1996) 398.
[5] M. Wittekind, M. Gorlach, M. Friedrichs, G. Dreyfuss and L. Mueller, Biochemistry, 31 (1992) 6254.
[6] A.L. Lee, R. Kanaar, D.C. Rio and D.E. Wemmer, Biochemistry, 33 (1994) 13775.
[7] C. Oubridge, N. Ito, P.R. Evans, C.-H. Teo and K. Nagai, Nature, 372 (1994) 432.
[8] B.M. Merrill, K.L. Stone, F. Cobianchi, S.H. Wilson and K.R. Williams, J. Biol. Chem., 263 (1988) 3307.
[9] W.T. Stump and K.B. Hall, RNA, 1 (1995) 55.
[10] D. Scherly, W. Boelens, W.J. van Venrooij, N.A. Dathan, J. Hamm and I. Mattaj, EMBO J., 8 (1989) 4163.
[11] D. Scherly, W. Boelens, N.A. Dathan, W.J. van Venrooij and I.W. Mattaj, Nature, 345 (1990) 502.
[12] C. Lutz-Freyermuth, C.C. Query and J.D. Keene, Proc. Natl. Acad. Sci. U.S.A., 97 (1990) 6393.
[13] W.C. Boelens, D. Scherly, P.R. Beijer, E.J.R. Jansen, N.A. Dathan, I.W. Mattaj and W. van Venrooij, Nucl. Acids Res., 19 (1991) 455.

[14] T.H. Jessen, C. Oubridge, C.H. Teo, C. Pritchard and K. Nagai, EMBO J., 10 (1991) 3447.
[15] J. Kranz, J. Lu and K.B. Hall, Protein Science, 5 (1996) 1567.
[16] W.T. Stump and K.B. Hall, RNA, 1 (1995) 55.
[17] K.B. Hall and W.T. Stump, Nucl. Acids Res., 20 (1992) 4283.
[18] M. Santoro and D.W. Bolen, Biochemistry, 27 (1988) 8063.
[19] C.N. Pace, Methods Enzymol., 131 (1986) 266.
[20] A. Tanaka, J. Flanagan and J.M. Sturtevant, Protein Science, 2 (1993) 567.
[21] C.N. Pace and K.E. Vanderburg, Biochemistry, 18 (1979) 288.
[22] M.M. Santoro and D.W. Bolen, Biochemistry, 31 (1992) 4901.
[23] G.T. Dekoster, A.D. Robertson, S.M. Stock and J.B. Stock, in R.H. Angeletti (Ed.), Techniques in Protein Chemistry IV, Academic Press Inc., San Diego, 1993, p. 533.
[24] C.N. Pace, D.V. Laurentsand and J.A. Thompson, Biochemistry, 29 (1990) 2564.
[25] I.J. Ropson, J.I. Gordon and C. Frieden, Biochemistry, 29 (1990) 9591.
[26] L. Swint and A.D. Robertson, Protein Science, 2 (1993) 2037.
[27] J. Lu and K.B. Hall, J. Mol. Biol., 247 (1995) 739.
[28] K.B. Hall, Biochemistry, 33 (1994) 10076.
[29] G.I. Makhatadze, G.M. Clore, A.M. Gronenborn and P.L. Privalov, Biochemistry, 33 (1994) 9327.
[30] C.W. van Gelder, F.J. Leusen, J.A. Leunissen and J.H. Noordik, Proteins Struct. Funct. Genetics, 18 (1994) 174–185.